

# Holothurian glycosaminoglycan inhibits metastasis via inhibition of P-selectin in B16F10 melanoma cells

Zhiqiang Yue<sup>1</sup> · Aiyun Wang<sup>1,2,3</sup> · Zhijie Zhu<sup>1</sup> · Li Tao<sup>1</sup> · Yao Li<sup>1</sup> ·  
Liang Zhou<sup>1</sup> · Wenxing Chen<sup>1,2,3</sup> · Yin Lu<sup>1,2,3</sup>

Received: 23 March 2015 / Accepted: 18 August 2015 / Published online: 30 August 2015  
© Springer Science+Business Media New York 2015

**Abstract** P-selectin-mediated tumor cell adhesion to platelets is a well-established stage in the process of tumor metastasis. Through computerized structural analysis, we found a marine-derived polysaccharide, holothurian glycosaminoglycan (hGAG), behaved as a ligand-competitive inhibitor of P-selectin, indicating its potential to disrupt the binding of P-selectin to cell surface receptor and activation of downstream regulators of tumor cell migration. Our experimental data demonstrated that hGAG significantly inhibited P-selectin-mediated adhesion of tumor cells to platelets and tumor cell migration in vitro and reduced subsequent pulmonary metastasis in vivo. Furthermore, abrogation of the P-selectin-mediated adhesion of tumor cells led to down-regulation of protein levels of integrins, FAK and MMP-2/9 in B16F10 cells, which is a crucial molecular mechanism of hGAG to inhibit tumor metastasis. In conclusion, hGAG has emerged as a novel anti-

cancer agent via blocking P-selectin-mediated malignant events of tumor metastasis.

**Keywords** Holothurian glycosaminoglycan · P-Selectin · Melanoma

## Introduction

Melanoma is the most aggressive type of skin cancer, and its incidence is rapidly increasing in all industrialized countries [1]. Because of local invasion and hematogenous metastasis, neither radiation therapy nor chemotherapy is able to substantially increase the length or quality of life of patients with advanced melanoma. Hematogenous metastasis is one of the major causes of mortality in melanoma patients and occurs as a complex multistep process involving cancer cell adhesion with platelets [2, 3]. Extensive experimental evidence shows that activated platelets promote tumor metastasis [4], which is important for tumor cell survival. Tumor cells in circulation interact with platelets and form tumor emboli that further contribute to tumor cell migration, extravasation, and the establishment of metastatic lesions [5]. Adhesive proteins expressed by platelets such as integrins and selectins enable the platelets to adhere to tumor cells that express their corresponding receptors [6]. Therefore, developing agents that effectively block or inhibit platelet and tumor cell adhesion would improve the treatment for melanoma metastasis [7].

Recently, increasing evidence indicates that P-selectin (CD62P) plays a critical role during hematogenous metastasis [8–11]. P-selectin has been shown to bind to several human cancers and human cancer-derived cell lines, such as human malignant melanoma [12], colon

Zhiqiang Yue and Aiyun Wang have contributed equally to this work.

**Electronic supplementary material** The online version of this article (doi:10.1007/s11010-015-2546-4) contains supplementary material, which is available to authorized users.

✉ Yin Lu  
profyinlu@163.com

<sup>1</sup> College of Pharmacy, Jiangsu Key Laboratory for Pharmacology and Safety Evaluation of Chinese Materia Medica, Nanjing University of Chinese Medicine, 138 Xianlin Road, Nanjing 210023, Jiangsu, China

<sup>2</sup> Jiangsu Collaborative Innovation Center of Traditional Chinese Medicine (TCM) Prevention and Treatment of Tumor, Nanjing 210023, China

<sup>3</sup> Jiangsu Provincial Center for Research and Development of Marine Drugs, Nanjing 210023, Jiangsu, China

cancer, lung cancer, breast cancer, and gastric cancer [13]. Studies demonstrate that P-selectin is an important mediator for the aggregation of activated platelets and cancer cells, facilitating in vivo tumor metastasis [14, 15] and the arrest of cancer cells [16]. Mechanistically, binding of P-selectin to tumor cell surface ligand regulates subsequent integrin-mediated steps in metastasis, which is critical for tumor emboli formation and metastasis [17]. Inhibiting selectin-mediated tumor cell interaction with blood constituents attenuates tumor metastasis in a number of animal models [18–21]. Therefore, blocking P-selectin interaction with tumor cells through antagonists can effectively inhibit tumor cell–platelet emboli complex formation and successfully prevent hematogenous metastasis [22, 23].

In clinic, there are several synthetic drug candidates targeting P-selectin, such as glycosaminoglycan compounds, including heparin and low-molecular-weight heparins [24]. Heparin is an excellent inhibitor of P-selectin, preventing P-selectin from binding to its natural ligands [25]. Addition of exogenous heparin competes for P-selectin binding and inhibits tumor cell adhesion processes. N-acetylated heparin reduces experimental melanoma metastasis through blocking P-selectin [26]. However, due to its strong anticoagulant potency, the application of P-selectin on anti-metastasis therapy is limited [27]. There are still medical needs to develop alternatives of heparin for anti-metastasis therapy.

In this study, we searched compounds targeting P-selectin in therapeutic targets database and DrugBank, and found that several compounds contain Glucosamine in the center of the molecular structure, similar to holothurian glycosaminoglycan (hGAG), a potential anti-metastasis compound suggested by our previous studies [28]. We discovered that heparin sodium and hGAG have similar characteristic peaks of infrared spectra, suggesting that they share similar structures. hGAG is a type of acidic mucopolysaccharide with average molecular weight of 114.802 kDa. It is extracted from the sea cucumber *Holothuria leucospilota* (Brand) [28, 29]. Similar to heparin, hGAG inhibits B16F10 melanoma metastasis in vivo, blocks tumor cell–platelet adhesion in vitro, reduces tumor cell migration mediated by activated platelets, and decreases integrin expression. However, the underlying mechanisms of hGAG to inhibit melanoma metastasis remain unknown.

Heparin possesses selectins' and integrins' inhibitory activity [6], and it inhibits tumor cell–platelet interactions mediated by P-selectin and mucins on tumor cell surface in vitro [25]. Since hGAG and heparin are structurally similar, we propose that hGAG can interfere the adhesion between tumor cells and platelet through blocking P-selectin binding.

To test this hypothesis and identify the target of hGAG, we applied computer virtual docking method to assess the binding activity of hGAG to P-selectin and other potential ligands that may play crucial role in tumor cell–platelet adhesion. Next, we assessed the inhibitory effect of hGAG on P-selectin and melanoma cells binding in vitro. Lastly, we tested the effect of hGAG on metastasis in vivo using an experimental metastasis mouse model.

Our results showed that hGAG exhibited higher binding activity with P-selectin than other proteins. We demonstrated that hGAG can inhibit the binding of melanoma B16F10 cells to P-selectin under static conditions and significantly inhibited P-selectin-mediated B16F10 cells' metastasis in our mouse model. These results indicate an anti-metastatic role for hGAG by disrupting P-selectin binding to tumor cells and subsequent tumor metastasis.

## Materials and methods

### Chemicals and reagents

Holothurian glycosaminoglycan (hGAG, purity > 98 %), purchased from Hualikang Biotechnology Co., Ltd (Changzhou, China), was dissolved in phosphate buffered saline (PBS) to prepare a stock solution (1 mM), filtered through 0.22  $\mu$ M membrane, and stored at  $-20^{\circ}\text{C}$ . Recombinant soluble human P-selectin-IgFc chimeric molecules (P-Fc) were obtained from Signalway Antibody LLC (SAB). The primary antibodies were anti-integrin  $\beta$ 3 (Chemicon) monoclonal antibody, anti-integrin  $\alpha$ 1 (Chemicon) monoclonal antibody, anti-FAK (SAB) monoclonal antibody, anti-MMP-2 (Bioworld), anti-MMP-9 (Bioworld), and Phospho-FAK (Tyr576/577) antibody (CST). The secondary antibodies were goat anti-Rabbit IgG (H&L)-HRP (Bioworld), and GAPDH (Sigma) was used as the internal control. A Supersignal kit was purchased from Millipore. BCA<sup>TM</sup> protein assay kit was purchased from Pierce.

### Cell lines and culture

B16F10 cells (ATCC) were maintained in DMEM supplemented with 10 % FBS. The cells were maintained in a humidified incubator ( $37^{\circ}\text{C}$ , 5 %  $\text{CO}_2$ ) and detached with 0.25 % Trypsin–0.02 % EDTA.

### Molecular docking

The X-ray crystal structures of proteins (P-selectin, GPIIb/IIIa, etc.) were obtained from RCSB Protein Data Bank (<http://www.rcsb.org>) and used as the basis of the docking

experiment. The structure of compound (hGAG) was drawn using ISIS-Draw and then exported in MOL format. The two-dimensional structures of hGAG and ligands were converted into three dimensional by small molecule-line structure transformation services. Schemes of hydrogen atoms and charges were added to the three-dimensional structure with an extensible molecular modeling system UCSF Chimera, which then were exported into mol2 format using Open Babel for further study of molecular docking.

The crystal structures of protein were used as the basis of the docking experiments. The active sites exploited in docking studies were defined as a subset region of 10.0 Å radius from the centroid of their ligands. Before screening, the docking protocol was validated. Each ligand was docked into the binding pocket to obtain the docked pose, and the root mean square deviation (RMSD) of all atoms between these two conformations was at 1.00 Å indicating that the parameters for docking simulation were good in reproducing the X-ray crystal structure.

Generally, about 10–100 individual docking simulations were performed, and interaction energy of each possible docking model was analyzed by AutoDock Tools (<http://www.mgltools.scripps.edu/>). After multiple docking simulations, consistent docking models among the best-fitted models were used for the development of the hypotheses.

### Size exclusion chromatography

Sephadex G-150 (Pharmacia) was suspended in five to tenfold volume of deionized (DI) water and heated to 50 °C for swelling and selectivity for specific molecular sizes; then chromatographic column was filled with fully swollen Sephadex by gentle stirring. After overnight balancing, Sephadex was saturated by elution buffer (DI water). hGAG (2 mg/ml) was incubated with or without 50 ng/ml recombinant P-selectin and loaded to the column. After the flow-through was collected, samples were sent for total carbohydrate analysis by a phenol–sulfuric acid method and the elution time was recorded.

### Flow cytometry

The experimental groups were prepared by combining 10 µl P-Fc (100 mg/ml) in PBS with 100 µl of hGAG at various concentrations. The control group was prepared by mixing 10 µl P-Fc with 100 µl 10 % BSA/PBS. All groups were incubated at room temperature (RT) for 30 min. Then, 100 µl of single cells were added to all groups and incubated for further 20 min. After centrifugation at 1000 r/min for 5 min, the cell pellets were collected and washed with PBS for three times. Then, 100 µl Rabbit-Anti-Human IgG–FITC (10 mg/ml) was added and the cells were

incubated for 1 h. The cells were collected by centrifugation at 1000 r/min for 5 min, and the pellets were washed with PBS for three times. Each aliquot of cells was resuspended with 0.5 ml PBS for immediate analysis by flow cytometry using a FACScan (BD Biosciences, Mountain View, CA).

### Tumor cell adhesion to immobilized P-Fc

96-well plates were coated with 10 µg/ml P-Fc and incubated at 4 °C overnight. The plates were then washed with PBS and blocked with 1 % bovine serum albumin (1 h, 37 °C). Confluent B16F10 plates were trypsinized, and the cells were harvested and diluted to a density of  $1 \times 10^6$ /ml. The cells were seeded onto 96-well plates and incubated with hGAG at 37 °C for 2 h. Plates were washed with PBS three times to remove unadhered cells. The attached cells were detected using hematoxylin and eosin (H & E) staining.

### Wound-healing mobility assay

B16F10 cells were seeded onto 6-well plates ( $5 \times 10^5$  cells/well) and allowed to grow to 90 % confluence in complete medium. The monolayers were wounded by scraping with P200 micropipette tips, and any cellular debris present was removed by gently washing with PBS. Cell monolayers were then incubated with serum-free medium containing 50 ng/ml P-selectin with various concentrations of hGAG for 24 h. Photographs of the exact wound regions were taken at the indicated time points (0 h and 24 h), at  $\times 100$  magnification.

### Transwell migration assay

B16F10 cell motility induced by P-selectin (50 ng/ml) was evaluated in a Transwell Boyden Chamber (Corning costar) with a polycarbonate filter (8-µm pores). Briefly, B16F10 cells ( $2 \times 10^5$  cells/ml) were added to the upper chamber containing hGAG (0–1 µM), while the lower chamber contained 600 µl DMEM with 50 ng/ml P-selectin or PBS (control). After incubation for 6 h at 37 °C, non-migrating cells were scrubbed off from the top of each filter, and the cells that had migrated to the lower surface of each filter were fixed in 70 % ethanol and stained with 0.1 % (w/v) crystal violet solution. Finally, the cells in five randomly selected microscopic fields ( $\times 100$ ) were counted. Three independent experiments were performed.

### Zebrafish tumor metastasis model

The zebrafish used in this study were housed in the zebrafish facility of the Model Animal Research Center (MARC), Nanjing University, AB/Tubingen (Germany)

strain, in accordance with IACUC-approved protocol (MARC-AP#: QZ01). Embryos were obtained from natural spawning of wild-type adults, and they were grown at  $28 \pm 1$  °C in embryo medium as previously described [30]. Twenty-four hours post-fertilization (24 hpf) zebrafish embryos were incubated with water containing 0.2 mM 1-phenyl-2-thio-urea (Sigma) to prevent pigmentation. 48 hpf zebrafish embryos were dechorionated with a sharp-tip forceps and anesthetized with 0.004 % (wt/vol) tricaine (Sigma). Before microinjection, monolayers of tumor cells at the proliferating phase were harvested and then stained with 2 µg/ml 1,1'-dioctadecyl-3,3,3',3'-tetramethylindocarbocyanine perchlorate (DiI, Invitrogen) as described [31]. After overnight recovery in culture medium, B16F10 cells were treated with or without P-selectin and hGAG for 2 h. Subsequently, cells were washed with DPBS, transferred to 1.5-ml tubes, and centrifuged for 3 min at 1000 rpm. The cells were then resuspended in DPBS at a concentration of  $2 \times 10^7$  cells/ml. Using a microloader (Eppendorf), the cell suspension was loaded into an injection needle (0.75 mm internal diameter and 1.0 mm external diameter). Approximately 100–200 tumor cells in 5 ml solution were injected into the perivitelline cavity of 48 hpf embryo using a microinjector (Narisshige). After injection, embryos were incubated for 1 h at 28.5 °C and checked for cell presence using a fluorescent microscope (Olympus MVX10). Embryos with fluorescent cells outside the implantation area were excluded to ensure that tumor cells are located only within the perivitelline space. 10 zebrafish embryos were included in each experimental group. All fish were incubated in housing-keeping water at 28.5 °C for 6 days. To measure the distance of metastasis, we chose the focus or cell that lied furthest away from the tumor mass and disseminated from the tumor mass toward the fish embryo head and measured the distance between that focus and the primary tumor using ImageJ [31].

### Western blot analysis

To detect protein expression of mucin-1,  $\beta 3$  and  $\alpha 1$  integrins, FAK, and MMP-2/9, B16F10 cells were treated with hGAG (0–1 µM) for 24 h or 48 h in the presence of P-selectin. Subsequently, cells were briefly washed with pre-cooled PBS and lysed in RIPA buffer (50 mM Tris-HCl, pH 7.4, 150 mM NaCl, 1 % NP-40, 0.1 % SDS, and 0.5 % sodium deoxycholate) supplemented with 1 mM PMSF, 1 µg/ml aprotinin, 1 µg/ml leupeptin, and 1 µg/ml pepstatin. Protein concentrations were determined using the BCA<sup>TM</sup> protein assay kit. Protein samples (50 µg/lane) were resolved by SDS-PAGE and transferred to a polyvinylidene difluoride membrane (Millipore). Proteins were detected by immunoblotting with the following antibodies: anti-integrin  $\beta 3$  monoclonal antibody, anti-integrin

$\alpha 1$  monoclonal antibody, anti-FAK monoclonal antibody, anti-MMP-2, anti-MMP-9, Phospho-FAK (Tyr576/577) antibody, Goat anti-Rabbit IgG (H&L)-HRP, and GAPDH, followed by incubation with corresponding secondary antibodies conjugated with horseradish peroxidase. A Supersignal kit was used to visualize the bands according to the manufacturer's instructions.

### Immunofluorescence analysis

The effects of hGAG on P-selectin-induced expression of mucin-1 in B16F10 cells were examined using an immunocytochemical method. Cells were seeded on glass coverslips and grew overnight, then pretreated with or without hGAG for 24 h in the presence of 50 ng/ml P-selectin. Following the treatment, the cells were fixed by pre-cold acetone for 30 min. After three times rinse with PBS, the cells were permeabilized in 0.1 % Triton X-100 and incubated with 1 % BSA/PBS to block nonspecific binding. Subsequently, anti-integrins and anti-mucin-1 antibodies or normal goat serum control were applied for immunofluorescent labeling, and goat anti-rabbit IgG-FITC (Boshide, Wuhan, China) was used as a secondary antibody. Fluorescence cells were observed and photographed under a laser scanning confocal microscope at  $\times 400$  magnification (LEICA TCS SP5, Mannheim, Germany).

### Experimental metastasis model, formation, and visualization of tumor cell–platelet complex in vivo

Female C57BL/6 mice (aged 6–8 weeks) were purchased from the Animal Resources Center of Nanjing Medical University (Nanjing, China). They were maintained in accordance with the Institutional Guides for the Care and Use of Laboratory Animals. Mice were housed in plastic cages under controlled temperature ( $22 \pm 2$  °C) and relative humidity ( $55 \pm 10$  %) with a 12-h light/12-h dark cycle (8:00–20:00) and were given unrestricted access to water and a commercial non-purified diet (Xietong Medicinal Bioengineering Co., Ltd, Nanjing, China). This study was approved by the Animal Research Ethics Committee of Nanjing University of Chinese Medicine.

The establishment of the experimental lung metastasis was performed as previously described. Overall, the suspension of B16F10 cells ( $2.5 \times 10^6$  cells in 0.2 ml normal saline per mouse) was injected through the tail vein of female C57BL/6 mice (6–8 weeks old) and allowed to create lung metastatic foci for 14 days. Mice were followed by an intraperitoneal administration of 26 mg/kg hGAG or PBS control each day. 14 days post tumor cell injection, all the mice were sacrificed and lungs were obtained and fixed by formalin. The lung metastasis foci were observed.

## Statistical analysis

Data were analyzed using one-way analysis of variance (GraphPad Prism 5, GraphPad Software Inc., San Diego, CA). The results are expressed as mean  $\pm$  SD of at least three independent experiments. The difference was considered significant between two samples if  $P < 0.05$ .

## Results

### hGAG has a high binding affinity to P-selectin

To identify the underlying mechanisms that mediate the inhibitory effects of hGAG on tumor cell adhesion to platelets, we applied molecular docking assay to screen the potential targets of hGAG among macromolecules that enhance cell aggregation and adhesion. hGAG exhibited the lowest interaction energy with P-selectin ( $-16.97$  kJ/mol) compared to other proteins such as TGF- $\beta$ , PDGF-B, TNF- $\alpha$ , vWF, platelet factor 4, GPIIb/IIIa, thrombin, and thromboxane A2 (Fig. S1; Table 1), which suggested that hGAG might preferably bind to P-selectin. We further found that hGAG interacted with P-selectin in the similar manner with P-selectin ligand Q14242, which formed one hydrogen bond with residues of P-selectin at active site residue ARG83 of 1G1R in our predicted binding mode (Fig. 1a). To verify the virtual data, we used size exclusion chromatography to investigate the binding affinity of the two molecules. Generally, high-molecular weight substances will be excluded from the Sephadex and are eluted first. As shown in Fig. 1b, the average elution time of hGAG was about 8 min. Surprisingly, the elution time approximately reduced to 3 min after incubating hGAG with P-selectin, which illustrated the formation of a larger intramolecular complex. Collectively, computer simulation and affinity test could predict the potential interactions between hGAG and P-selectin.

### hGAG inhibits P-selectin binding to B16F10 cells

To validate whether P-selectin is involved in hGAG-mediated disruption of the interactions between tumor cells and platelets and subsequently inhibition of metastasis, we used competitive binding test to verify hGAG as a potential antagonist of P-selectin by FACS analysis. Our results showed that the recombinant P-selectin peptide (P-Fc)

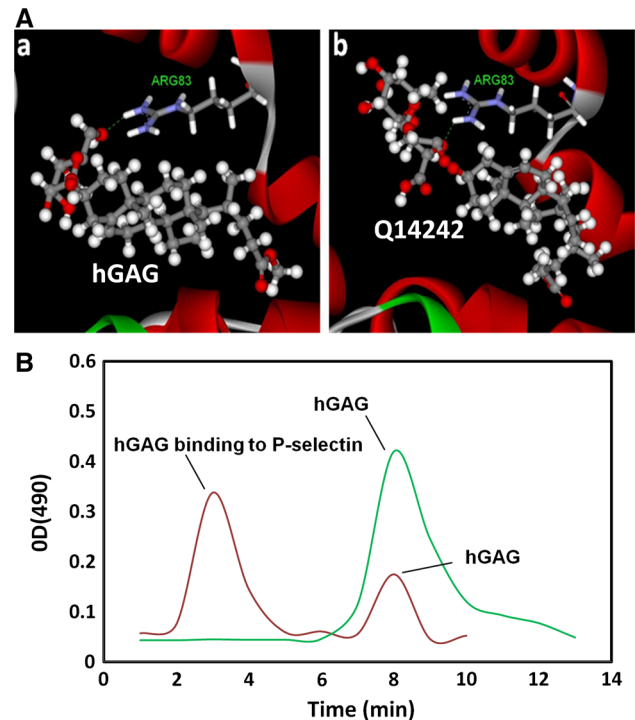


**Fig. 1** Diagram of hGAG binding to P-selectin. **a** hGAG and P-selectin ligand docked in the pocket of P-selectin. Putative hydrogen bonds between hGAG (**a**) or Q14242 (**b**, the ligand of P-selectin) and P-selectin are shown in green dashes, ligands shown in ball and stick fashion, and P-selectin's active residues shown in lines. **b** Size exclusion chromatography for analyzing the potential affinity of hGAG to P-selectin. The green elution curve was the elution profile of hGAG, while the red elution curve was that after incubation with P-selectin. (Color figure online)

could significantly bind to the cell surface of B16F10, exhibiting a positive population of FITC-staining cells, while hGAG dramatically decreased the percentage of cells combined with soluble P-Fc (Fig. 2a). Furthermore, we also fixed P-Fc on the cell culture plates, leaving B16F10 cells freely binding to the immobilized P-Fc. As shown in Fig. 2b, hGAG dose dependently attenuated the adhesion of tumor cells to the immobilized P-F, and 1  $\mu$ M of hGAG could totally reverse the tumor cells to the background level ( $P < 0.01$ ). Altogether, these findings confirmed that hGAG might be a potential competitive inhibitor of P-selectin and it subsequently abolished P-selectin binding to the tumor cell surface. Therefore, we further speculated that hGAG might block the ligand behavior of P-selectin as an initiator of intracellular signaling pathways that leading to malignant phenotypes of tumor cell.

**Table 1** Theoretical affinity of hGAG and ligand with respect to P-selectin (1G1R)

Ligand	Binding score	H-bonding	Number of hydrogen bonds	Residues
hGAG	$-16.97$	$-6.89$	1	ARG83:N-HO36
Q14242	$-17.31$	$-7.05$	1	ARG83:N-HO1

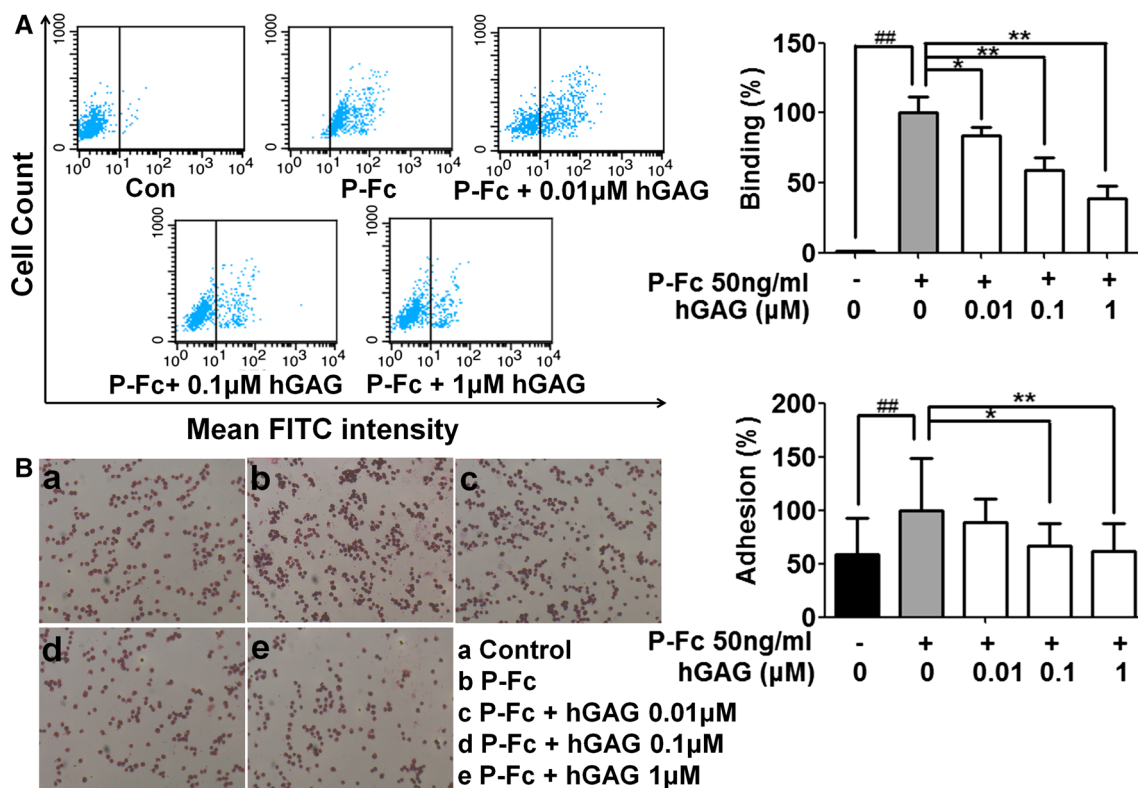


**Fig. 2** hGAG inhibits P-selectin binding to B16F10 cells in vitro. **a** hGAG inhibits P-Fc binding to B16F10 cells. P-Fc was pre-incubated with hGAG or PBS and then added to B16F10 monolayers. P-Fc was detected by Rabbit-Anti-Human IgG-FITC. The binding events were analyzed by flow cytometry as described. **b** hGAG inhibits B16F10 cells binding to immobilized P-selectin. The graph represents the relative percentages of hGAG that inhibited B16F10

cells binding to immobilized P-Fc in vitro. For each condition, five random fields were counted. Data are expressed as the mean  $\pm$  SD (*a*, *n* = 5; *b*, *n* = 9),  $^{###}P < 0.01$  P-Fc treatment alone group compared to control group without P-Fc and hGAG treatment by one-way ANOVA,  $^{*}P < 0.05$ ,  $^{**}P < 0.01$ , P-Fc treatment groups with various hGAG treatment compared to P-Fc treatment alone group by two-way ANOVA

### hGAG inhibits P-selectin-induced B16F10 tumor cell migration in vitro and metastasis in vivo

To further examine whether hGAG could inhibit P-selectin-activated cell motility, we used wound-healing and Transwell migration models in the absence or the presence of hGAG and P-selectin. As a result, we found that P-selectin increased the horizontal migration of B16F10 cells significantly in wound-healing assay ( $P < 0.01$ ), which was inhibited by hGAG in a dose-dependent manner (Fig. 3a). We found that non-cytotoxic doses of hGAG also induced a dose-dependent inhibition of B16F10 cells' vertical migration using transwell migration model. Significantly, 1 μM of hGAG inhibited 58.48 % of B16F10 cell migration in the visible fields (Fig. 3b). After that, we then investigated the role of the hGAG on P-selectin-mediated tumor cell invasion, dissemination, and metastasis in zebrafish model. The metastatic B16F10 tumor cells were treated with or without P-selectin and then treated with 1 μM of hGAG. Tumor cells were labeled with DiI and then injected into the perivitelline cavity of 48 h post-

fertilization zebrafish embryos. Notably, as shown in Fig. 3c, at day 6 after tumor implantation, the fish embryo injected with P-selectin alone exerted evident hematogenous metastasis far away from the injection site, while hGAG effectively suppressed the process in tumor-bearing fish embryos.

### hGAG down-regulates P-selectin-induced activation of integrin-FAK signals and expression of MMPs

It has been shown that P-selectin increases the expression of MMPs, integrins, and FAK, thus enhancing integrin-mediated tumor cell metastasis. Therefore, we examined the levels of downstream regulators of P-selectin that is incubated with or without hGAG. Initially, we found that hGAG could interrupt P-selectin-mediated activation of integrin-FAK signaling pathway. The underlying mechanism might be related to the down-regulation of membrane-embedded integrin  $\beta 3$  (Fig. 4a). The immunofluorescence staining of integrins also support the evidence. Furthermore, hGAG also inhibited the expression of MMP-2 and MMP-9 under 48 h

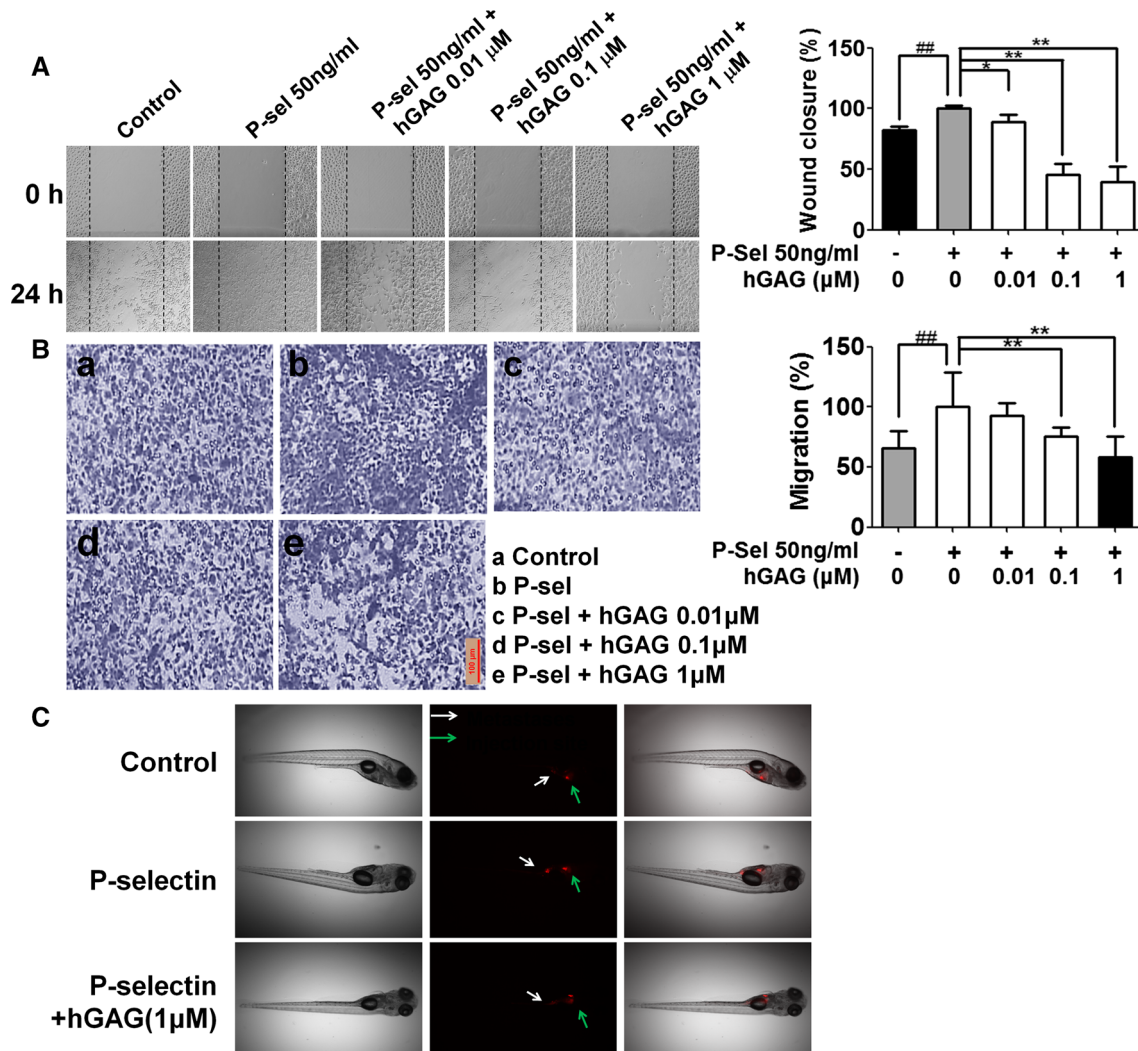


**Fig. 3** hGAG inhibits P-selectin-induced B16F10 tumor cell migration in vitro and metastasis in vivo. **a** hGAG inhibited P-selectin-induced mobility of B16F10 cells by wound-healing assay. A single wound was created in the center of 90 % confluence B16F10 cell monolayer, and cell debris was removed by washing. After 24 h of incubation, wound closure was visualized under an inverted microscope at  $\times 100$  magnification. Phase contrast images were taken at 0 and 24 h after wounding and wound closure percent was quantified using ImageJ software. **b** hGAG inhibited P-selectin-induced mobility of B16F10 cells by transwell migration assay. B16F10 cells treated

with hGAG were allowed to migrate for 6 h towards media containing P-selectin (50 ng/ml). After 6 h, cells that migrated to the bottom of the filters were stained with crystal violet and micrographs were taken at  $\times 100$  magnification. Scale bar represents 100  $\mu$ m. **c** Effect of hGAG on tumor metastasis in vivo. Tumor cells labeled with DiI were injected into the perivitelline cavity of 48 h post-fertilization zebrafish embryos. At day 6 after implantation, B16F10 tumor cell metastasis was detected by assaying DiI fluorescence using a laser scanning confocal microscope

of drug exposure. Taken together, inhibition of P-selectin-mediated activation of integrin–FAK signaling pathways and expression of MMPs by hGAG accounted for the lower aggressive metastatic tendency.

### hGAG inhibits experimental melanoma lung metastasis

In order to visualize the decreased lung nodules with less tumor emboli by hGAG, mice were pretreated with or without single-dose hGAG (26 mg/kg) in experimental

melanoma lung metastasis model. B16F10 cells were injected intravenously via the tail vein into C57/BL6 mice. 14 days later, the lung tissues were harvested at the end time point. As shown in the representative photos in Fig. 5a, b, the number of lung metastasis foci decreased significantly in mice with the treatment of 26 mg/kg hGAG compared to vehicle control ( $P < 0.01$ ). Immunohistochemical staining showed that hGAG could down-regulate the expression of integrin  $\beta 3$  in the lung foci (Fig. 5c). Therefore, mice bearing metastases could respond to hGAG treatment with disrupted tumor emboli formation.

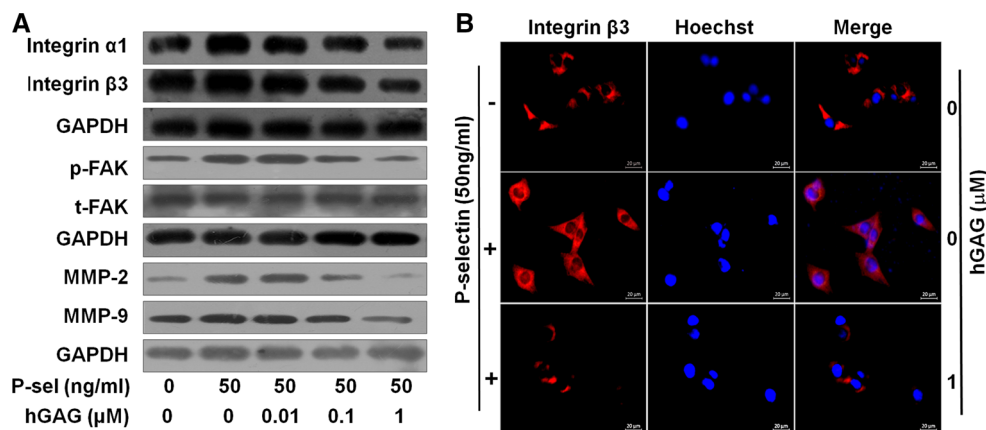


**Fig. 4** hGAG down-regulates P-selectin-induced MMPs, integrins, and FAK expression. **a** hGAG down-regulates protein levels of P-selectin-induced integrin  $\alpha 1$ ,  $\beta 3$ , and FAK expression in B16F10 melanoma cells. **b** B16F10 cells were treated with hGAG (1  $\mu$ M) with or without P-selectin (50 ng/ml), then cells were fixed and incubated

with primary antibodies against Integrin  $\beta 3$ . Cells were immunostained with anti-rabbit FITC-conjugated secondary antibody and then stained with Hoechst 33258. The specimens were visualized and photographed using a fluorescence microscope ( $\times 400$ , scale bar represents 20  $\mu$ m)

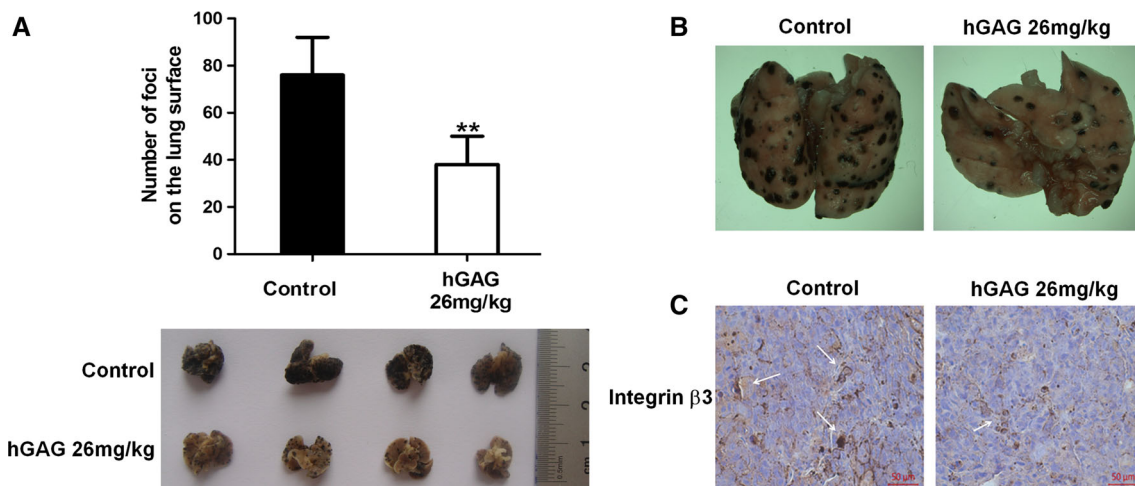


**Fig. 5** hGAG inhibits tumor metastasis in a mouse lung melanoma metastasis model. **a** C57BL/6 mice were injected with  $2.5 \times 10^6$  B16F10 cells and administrated with hGAG (26 mg/kg) for 14 days. The mice then were sacrificed and lungs were obtained for observation and quantification of pulmonary intravascular metastases

formation. **b** Representative lungs with experimental pulmonary melanoma foci were from mice treated with saline (control) and hGAG (26 mg/kg), respectively. **c** Immunohistochemical staining of integrin  $\beta 3$  expression in the lung of mice treated with and without hGAG

### Cell-surface PSGL-1 (mucin-1) is not affected by hGAG

P-selectin mainly binds to a mucin-type glycoprotein PSGL-1 (P-selectin glycoprotein ligand-1) or mucin-1 on tumor cells to activate downstream signal pathways [32, 33]. Our data show that hGAG treatment did not change the expression level of mucin-1. As shown in Fig. 6a, neither hGAG nor P-selectin (50 ng/ml) had any obvious effect on protein levels of mucin-1 after treated for 24 h by Western blot analysis. The result was confirmed by immunofluorescence staining of mucin-1 on B16F10 cells (Fig. 6b).

Our results suggest that hGAG functions as a competitive inhibitor to prevent P-selectin from binding to its ligands such as mucin-1, but is not involved in reducing ligand protein levels.

### Discussion

In this study, we have shown that hGAG had anti-metastatic properties possibly via inhibition of P-selectin binding to tumor cells as a ligand antagonist of P-selectin and suppression of adhesion and migration ability of cancer cells, by



down-regulating  $\beta_3$  integrin and FAK (Fig. 7). Our findings suggest that hGAG as a valuable candidate could potentially be exploited to inhibit tumor metastasis.

P-selectin is a member of selectin family of cell adhesion molecules that facilitates interactions among tumor cells, platelets, and endothelial cells [34]. Expressed on

activated endothelial cells and thrombin-activated platelets [35–37], P-selectin binding to melanoma cells specifically activates integrins, which results in the increase of cell migration and cell attachment to extracellular matrix (ECM) [38]. The increase in expression of  $\beta_3$  and  $\beta_1$  integrins has been shown to correlate with increased

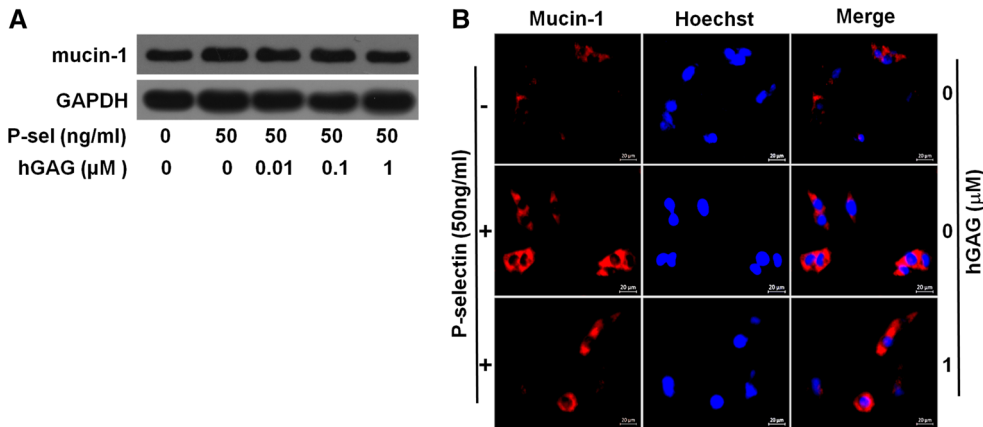


**Fig. 6** hGAG treatment shows no effect on the expression of mucin-1. **a** B16F10 cells were treated with hGAG (0, 0.01, 0.1, and 1  $\mu$ M) for 24 h in the presence or absence of P-selectin, and then cells were collected. The mucin-1 expression was analyzed with Western blot, and GAPDH was used as a loading control. **b** B16F10 cells were

seeded on coverslips and treated with PBS (control) or hGAG at 0 and 1  $\mu$ M for 24 h at 37 °C in the presence or absence of P-selectin. The mucin-1 expression was detected by immunofluorescence (red), and cell nuclei were labeled with Hoechst 33258 (blue). Scale bar represents 20  $\mu$ m. (Color figure online)

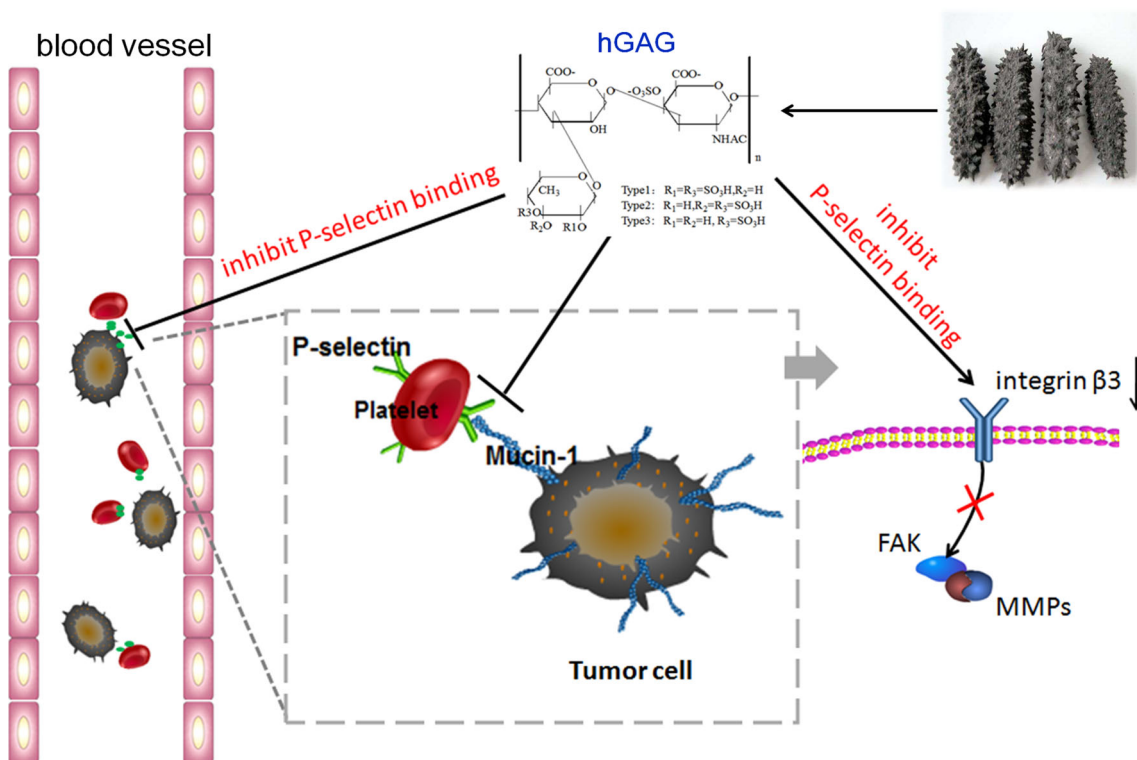


**Fig. 7** Proposed model by which hGAG inhibits tumor metastasis. hGAG prevents P-selectin from binding to its receptor and attenuates P-selectin-mediated interaction of platelets and tumor cells, leading to

deactivation of integrin–MMPs signaling and reduced levels of lung metastasis

P-selectin level. It is believed that dysregulation of integrin-mediated cell adhesion and migration contributes to the increase of the metastatic process [39]. FAK is a focal adhesion-associated protein kinase involved in cellular adhesion. Activated integrin activates FAK pathway, thus regulating tumor cell adhesion and migration [40, 41]. It had been shown that when FAK was inhibited, cancer cells became less metastatic due to decreased mobility [42]. P-selectin binding to mucin-1 on cancer cells activates signals that promote tumor cell adhesion and migration [32]. Consequently, P-selectin inhibition might have a beneficial effect on cancer therapies by attenuating both tumor cell migration and adhesion [35]. There are abundant experimental data indicating that heparins attenuate metastasis by interfering P-selectin interaction with tumor cell [25, 43–46]. However, heparin therapy can be difficult to administrate on an outpatient basis and is associated with complications [25]. In the current study, we demonstrated that hGAG, which is very close to heparin structurally, may prevent or disrupt the processes of P-selectin-mediated metastasis. It is quite true that the anti-metastasis effects mediated by heparin are both dependent and independent on its anticoagulant properties. hGAG also exhibits dual mechanisms. Previously, we found that an essential target of hGAG might be tissue factor (TF), the initiator of extrinsic pathway of coagulation [28]. However, in this study, we considered that the anticoagulant feature of hGAG was not involved. Heparin can attenuate tumor metastasis mainly due to inhibition of P-selectin, but non-anticoagulant heparins also have similar effects. Instead of heparin, low-molecular weight heparin (LMWH) with decreased anticoagulant properties can eliminate the major side effects of heparin in cancer treatment [47, 48]. Therefore, we believed that the inhibition of P-selectin was the primary mechanism of hGAG to reduce tumor hematogenous metastasis.

In addition to heparin, another glycosaminoglycan, namely fucosylated chondroitin sulfate (FucCS), has been proven to be a potent inhibitor of selectins. Both hGAG and FucCS are acid mucopolysaccharides with high molecular weight from sea cucumber. hGAG was isolated from *Holothuria leucospilota*, while FucCS was from *Ludwigothurea grisea*. The major structure differences exist in the percentage and position of sulfated residues. The backbone of hGAG consists of repeating disaccharide units of  $\beta$ -D-glucuronic acid and *N*-acetyl- $\beta$ -D-glucosamine, but *N*-acetyl- $\beta$ -D-glucosamine is 6-carboxylated, while that of FucCS is 6-sulfated [46]. It is reported that fucosylated sialylated glycans such as sialyl Lewis  $\times$  (sLe<sup>x</sup>) is essential for interaction between selectin family of adhesion molecules and their glycosylated ligands [49]. SLe<sup>x</sup> mimics that contain the essential functional groups for receptor interaction and a negative charge or a hydrophobic group have

been developed as inhibitors of E-, P-, and L-selectins [50]. hGAG is a nature-derived glycosaminoglycan or mucopolysaccharide, emerged as a structural and functional mimic of SLe<sup>x</sup>, and is postulated to be able to compete with SLe<sup>x</sup> binding to P-selectin. The potential side effects of hGAG have not been well documented yet, but the anti-P-selectin activity of hGAG might induce the deficiency of platelet function and related disorders. Therefore, a more comprehensive assessment of in vivo safety is critical for the future application of hGAG as an anti-P-selection agent in cancer prevention and treatment.

In summary, we dissected out the three potential mechanisms of hGAG to inhibit metastasis. Our findings demonstrated that hGAG had a high potential in vitro to (a) inhibit P-selectin-induced melanoma B16F10 cell migration and mobility; (b) down-regulate the expression of  $\beta$ 3 integrins and FAK at protein levels in B16F10 cells; and (c) inhibit B16F10 cell migration and adhesion through blocking P-selectin binding to tumor cells. Each of these effects appears to contribute to the inhibition of metastasis of melanoma.

**Acknowledgments** This Project was supported in part by National Natural Science Foundation of China (Nos. 81173174, 81202655), Doctoral Program of the Ministry of Education (20113237110008), 2013' Program for Excellent Scientific and Technological Innovation Team of Jiangsu Higher Education, Jiangsu Ordinary University Graduate Students Scientific Research Innovation Program (CXLX11-0772), and a project of the Priority Academic Program Development of Jiangsu Higher Education Institutions (PAPD).

#### Compliance with ethical standards

**Conflict of interest** The authors declare that no competing interests exist.

## References

1. Das Thakur M, Salangsang F, Landman AS, Sellers WR, Pryer NK, Levesque MP, Dummer R, McMahon M, Stuart DD (2013) Modelling vemurafenib resistance in melanoma reveals a strategy to forestall drug resistance. *Nature* 494(7436):251–255
2. Mervic L (2012) Time course and pattern of metastasis of cutaneous melanoma differ between men and women. *PLoS One* 7(3):e32955
3. Erpenbeck L, Schon MP (2010) Deadly allies: the fatal interplay between platelets and metastasizing cancer cells. *Blood* 115(17):3427–3436
4. Gay LJ, Felding-Habermann B (2011) Contribution of platelets to tumour metastasis. *Nat Rev Cancer* 11(2):123–134
5. Tsuruo T, Fujita N (2008) Platelet aggregation in the formation of tumor metastasis. *Proc Jpn Acad Ser B Phys Biol Sci* 84(6):189–198
6. Bendas G, Borsig L (2012) Cancer cell adhesion and metastasis: selectins, integrins, and the inhibitory potential of heparins. *Int J Cell Biol* 2012:676731
7. Bambace NM, Holmes CE (2011) The platelet contribution to cancer progression. *J Thromb Haemost* 9(2):237–249

8. Chen C, He Z, Sai P, Faridi A, Aziz A, Kalavar M, Grieciene P, Gintautas J, Steier W (2004) Inhibition of human CD24 binding to platelet-bound P-selectin by monoclonal antibody. *Proc West Pharmacol Soc* 47:28–29
9. Garcia J, Callewaert N, Borsig L (2007) P-selectin mediates metastatic progression through binding to sulfatides on tumor cells. *Glycobiology* 17(2):185–196
10. Mi D, Gao Y, Zheng S, Ba X, Zeng X (2009) Inhibitory effects of chemically modified heparin on the P-selectin-mediated adhesion of breast cancer cells in vitro. *Mol Med Rep* 2(2):301–306
11. Raman PS, Alves CS, Wirtz D, Konstantopoulos K (2011) Single-molecule binding of CD44 to fibrin versus P-selectin predicts their distinct shear-dependent interactions in cancer. *J Cell Sci* 124(Pt 11):1903–1910
12. Ma YQ, Geng JG (2000) Heparan sulfate-like proteoglycans mediate adhesion of human malignant melanoma A375 cells to P-selectin under flow. *J Immunol* 165(1):558–565
13. Ferroni P, Roselli M, Martini F, D'Alessandro R, Mariotti S, Basili S, Spila A, Aloe S, Palmirotta R, Maggini A, Del Monte G, Mancini R, Graziano F, Cosimelli M, Guadagni F (2004) Prognostic value of soluble P-selectin levels in colorectal cancer. *Int J Cancer* 111(3):404–408
14. Qi CL, Wei B, Ye J, Yang Y, Li B, Zhang QQ, Li JC, He XD, Lan T, Wang LJ (2014) P-selectin-mediated platelet adhesion promotes the metastasis of murine melanoma cells. *PLoS One* 9(3):e91320
15. Chen M, Geng JG (2006) P-selectin mediates adhesion of leukocytes, platelets, and cancer cells in inflammation, thrombosis, and cancer growth and metastasis. *Arch Immunol Ther Exp* 54(2):75–84
16. Reyes-Reyes EM, Akiyama SK (2008) Cell-surface nucleolin is a signal transducing P-selectin binding protein for human colon carcinoma cells. *Exp Cell Res* 314(11–12):2212–2223
17. Reyes-Reyes ME, George MD, Roberts JD, Akiyama SK (2006) P-selectin activates integrin-mediated colon carcinoma cell adhesion to fibronectin. *Exp Cell Res* 312(20):4056–4069
18. Kim YJ, Borsig L, Varki NM, Varki A (1998) P-selectin deficiency attenuates tumor growth and metastasis. *Proc Natl Acad Sci USA* 95(16):9325–9330
19. Borsig L, Wong R, Hynes RO, Varki NM, Varki A (2002) Synergistic effects of L- and P-selectin in facilitating tumor metastasis can involve non-mucin ligands and implicate leukocytes as enhancers of metastasis. *Proc Natl Acad Sci USA* 99(4):2193–2198
20. Laubli H, Stevenson JL, Varki A, Varki NM, Borsig L (2006) L-selectin facilitation of metastasis involves temporal induction of Fut7-dependent ligands at sites of tumor cell arrest. *Cancer Res* 66(3):1536–1542
21. Laubli H, Borsig L (2010) Selectins as mediators of lung metastasis. *Cancer Microenviron* 3(1):97–105
22. Gao Y, Wei M, Zheng S, Ba X, Hao S, Zeng X (2006) Chemically modified heparin inhibits the in vitro adhesion of non-small cell lung cancer cells to P-selectin. *J Cancer Res Clin Oncol* 132(4):257–264
23. Kozlowski EO, Pavao MS, Borsig L (2011) *Ascidian dermatan* sulfates attenuate metastasis, inflammation and thrombosis by inhibition of P-selectin. *J Thromb Haemost* 9(9):1807–1815
24. Sasisekharan R, Shriver Z, Venkataraman G, Narayanasami U (2002) Roles of heparan-sulphate glycosaminoglycans in cancer. *Nat Rev Cancer* 2(7):521–528
25. Borsig L, Wong R, Feramisco J, Nadeau DR, Varki NM, Varki A (2001) Heparin and cancer revisited: mechanistic connections involving platelets, P-selectin, carcinoma mucins, and tumor metastasis. *Proc Natl Acad Sci USA* 98(6):3352–3357
26. Schlesinger M, Roblek M, Ortmann K, Naggi A, Torri G, Borsig L, Bendas G (2014) The role of VLA-4 binding for experimental melanoma metastasis and its inhibition by heparin. *Thromb Res* 133(5):855–862
27. Li Y, Luo JY, Cui HF, Zheng L, Du SS (2010) Study on anti-metastasis of heparin derivatives as ligand antagonist of p-selectin. *Biomed Pharmacother* 64(10):654–658
28. Zhao Y, Zhang D, Wang S, Tao L, Wang A, Chen W, Zhu Z, Zheng S, Gao X, Lu Y (2013) Holothurian glycosaminoglycan inhibits metastasis and thrombosis via targeting of nuclear factor-kappaB/tissue factor/factor Xa pathway in melanoma B16F10 cells. *PLoS One* 8(2):e56557
29. Zhang W, Lu Y, Xu B, Wu J, Zhang L, Gao M, Zheng S, Wang A, Zhang C, Chen L, Lei N (2009) Acidic mucopolysaccharide from *Holothuria leucospilota* has antitumor effect by inhibiting angiogenesis and tumor cell invasion in vivo and in vitro. *Cancer Biol Ther* 8(15):1489–1499
30. Liang D, Jia W, Li J, Li K, Zhao Q (2012) Retinoic acid signaling plays a restrictive role in zebrafish primitive myelopoiesis. *PLoS One* 7(2):e30865
31. Rouhi P, Jensen LD, Cao Z, Hosaka K, Lanne T, Wahlberg E, Steffensen JF, Cao Y (2010) Hypoxia-induced metastasis model in embryonic zebrafish. *Nat Protoc* 5(12):1911–1918
32. McDermott KM, Crocker PR, Harris A, Burdick MD, Hinoda Y, Hayashi T, Imai K, Hollingsworth MA (2001) Overexpression of MUC1 reconfigures the binding properties of tumor cells. *Int J Cancer* 94(6):783–791
33. Xu J, Cai J, Anderson B, Wagner B, Albrecht R, Peek SF, Suresh M, Darien BJ (2007) Cloning and functional characterization of recombinant equine P-selectin. *Vet Immunol Immunopathol* 116(3–4):115–130
34. Hostettler N, Naggi A, Torri G, Ishai-Michaeli R, Casu B, Vladavsky I, Borsig L (2007) P-selectin- and heparanase-dependent antimetastatic activity of non-anticoagulant heparins. *FASEB J* 21(13):3562–3572
35. Ludwig RJ, Schon MP, Boehncke WH (2007) P-selectin: a common therapeutic target for cardiovascular disorders, inflammation and tumour metastasis. *Expert Opin Ther Targ* 11(8):1103–1117
36. Barkalow FJ, Barkalow KL, Mayadas TN (2000) Dimerization of P-selectin in platelets and endothelial cells. *Blood* 96(9):3070–3077
37. Koedam JA, Cramer EM, Briend E, Furie B, Furie BC, Wagner DD (1992) P-selectin, a granule membrane protein of platelets and endothelial cells, follows the regulated secretory pathway in ArT-20 cells. *J Cell Biol* 116(3):617–625
38. Felding-Habermann B, Habermann R, Saldivar E, Ruggeri ZM (1996) Role of beta3 integrins in melanoma cell adhesion to activated platelets under flow. *J Biol Chem* 271(10):5892–5900
39. Shin S, Wolgamott L, Yoon SO (2012) Integrin trafficking and tumor progression. *Int J Cell Biol* 2012:516789
40. Shibue T, Weinberg RA (2009) Integrin beta1-focal adhesion kinase signaling directs the proliferation of metastatic cancer cells disseminated in the lungs. *Proc Natl Acad Sci USA* 106(25):10290–10295
41. Mitra SK, Schlaepfer DD (2006) Integrin-regulated FAK-Src signaling in normal and cancer cells. *Curr Opin Cell Biol* 18(5):516–523
42. Golubovskaya VM (2010) Focal adhesion kinase as a cancer therapy target. *Anti-Cancer Agents Med Chem* 10(10):735–741
43. Varki A, Varki NM (2001) P-selectin, carcinoma metastasis and heparin: novel mechanistic connections with therapeutic implications. *Braz J Med Biol Res* 34(6):711–717
44. Varki NM, Varki A (2002) Heparin inhibition of selectin-mediated interactions during the hematogenous phase of carcinoma metastasis: rationale for clinical studies in humans. *Semin Thromb Hemost* 28(1):53–66
45. Wei M, Tai G, Gao Y, Li N, Huang B, Zhou Y, Hao S, Zeng X (2004) Modified heparin inhibits P-selectin-mediated cell adhesion

- of human colon carcinoma cells to immobilized platelets under dynamic flow conditions. *J Biol Chem* 279(28):29202–29210
46. Borsig L, Wang L, Cavalcante MC, Cardilo-Reis L, Ferreira PL, Mourao PA, Esko JD, Pavao MS (2007) Selectin blocking activity of a fucosylated chondroitin sulfate glycosaminoglycan from sea cucumber. Effect on tumor metastasis and neutrophil recruitment. *J Biol Chem* 282(20):14984–14991
47. Stevenson JL, Varki A, Borsig L (2007) Heparin attenuates metastasis mainly due to inhibition of P- and L-selectin, but non-anticoagulant heparins can have additional effects. *Thromb Res* 120(Suppl 2):S107–S111
48. Borsig L (2007) Antimetastatic activities of modified heparins: selectin inhibition by heparin attenuates metastasis. *Semin Thromb Hemost* 33(5):540–546
49. Stone JP, Wagner DD (1993) P-selectin mediates adhesion of platelets to neuroblastoma and small cell lung cancer. *J Clin Invest* 92(2):804–813
50. Wong CH, MorisVara F, Hung SC, Marron TG, Lin CC, Gong KW, WeitzSchmidt G (1997) Small molecules as structural and functional mimics of sialyl Lewis X tetrasaccharide in selectin inhibition: a remarkable enhancement of inhibition by additional negative charge and/or hydrophobic group. *J Am Chem Soc* 119(35):8152–8158